Available at www.sciencedirect.com

SCIENCE DIRECT®

journal homepage: www.elsevier.com/locate/watres

Surfactant effects on α-factors in aeration systems

*Diego Rosso**, *Michael K. Stenstrom*

Civil and Environmental Engineering Department, University of California, Los Angeles, CA 90095-1593, USA

ARTICLE INFO

Article history:
Received 9 August 2005
Received in revised form
9 January 2006
Accepted 30 January 2006

Keywords:
Aeration
α-factor
Efficiency
Gas–liquid interface
Oxygen transfer
Surfactant

ABSTRACT

Aeration in wastewater treatment processes accounts for the largest fraction of plant energy costs. Aeration systems function by shearing the surface (surface aerators) or releasing bubbles at the bottom of the tank (coarse- or fine-bubble aerators). Surfactant accumulation on gas–liquid interfaces reduces mass transfer rates, and this reduction in general is larger for fine-bubble aerators. This study evaluates mass transfer effects on the characterization and specification of aeration systems in clean and process water conditions. Tests at different interfacial turbulence regimes show higher gas transfer depression for lower turbulence regimes. Contamination effects can be offset at the expense of operating efficiency, which is characteristic of surface aerators and coarse-bubble diffusers. Results describe the variability of α-factors measured at small scale, due to uncontrolled energy density. Results are also reported in dimensionless empirical correlations describing mass transfer as a function of physiochemical and geometrical characteristics of the aeration process.

1. Introduction

Aeration is an essential process in the majority of wastewater treatment plants and accounts for the largest fraction of plant energy costs, ranging from 45% to 75% of the plant energy expenditure (Reardon, 1995). Aeration systems transfer oxygen into a liquid media by either diffusing gas through a gas–liquid interface, or dissolving gas into the liquid solution using a semi-permeable membrane. Environmental technologies usually rely on interfacial gas transfer, with a gas–liquid interface created by either shearing the liquid surface with a mixer or turbine, or by releasing air through spargers or porous materials. Surface aerators shear the wastewater surface producing a spray of fine droplets that land on the wastewater surface within few seconds and over a radius of a few metres. Diffusers are nozzles or porous surfaces placed on the tank bottom that release bubbles travelling towards the tank surface. In general, bubbles are considered fine when their diameters are less than 5 mm. Coarse bubbles are larger, customarily produced by orifices 6 mm and larger (WEF, 1991), and may have diameters as large as 50 mm. Falling droplets and rising coarse bubbles have large interfacial gas–liquid velocity gradients and can be grouped as high-flow regime interfaces, whereas fine bubbles have low interfacial velocity gradients and can be grouped as low-flow regime interfaces.

Polymeric or ceramic porous sintered materials and polymeric punched membranes are usually grouped together and referred to as fine-pore diffusers. There exists other aeration equipment, such as submerged turbines or jet diffusers, which can create fine bubbles without using small orifices, and are fine-bubble but not fine-pore aerators. These technologies use mechanical energy to shear large bubbles into fine bubbles. Novel devices (referred to as bubbleless) utilize the intrinsic porosity of "true" semi-permeable membranes, such as reverse osmosis membranes, for transferring gas into the liquid. These membranes allow the transit of water and air across the membrane, without permitting the passage of solute or suspended matter and without generating an interface (Côté et al., 1989).

*Corresponding author. Tel.: +1 310 825 1408; fax: +1 310 206 5476.
E-mail address: bidui@ucla.edu (D. Rosso).
0043-1354/$ - see front matter © 2006 Elsevier Ltd. All rights reserved.
doi:10.1016/j.watres.2006.01.044

Fine-pore diffusers have become the most common aeration technology in wastewater treatment in developed countries. They have higher efficiencies per unit energy consumed (standard aeration efficiency or SAE, kg_{O_2}/kWh), and are usually installed in full floor configurations, which enhance their operating efficiency. Fine-pore diffusers have two important disadvantages: the need for periodic cleaning and the large negative impact on transfer efficiency from wastewater contaminants. The implications of fine-pore diffuser ageing and the benefits of cleaning have been previously discussed (Rosso and Stenstrom, 2006).

The impact of contamination on aeration performance is usually quantified by the α-factor (ratio of process water to clean water mass transfer coefficients, or k_La_{pw}/k_La_{cw}) (Stenstrom and Gilbert, 1981). Lower flow regime gas–liquid interfaces (such as the ones produced by fine-pore diffusers) generally have lower α than higher flow regime interfaces (such as the ones produced by coarse-bubble diffusers or surface aerators) for similar conditions (Stenstrom and Gilbert, 1981). Differences in α amongst aeration systems were noted in the 1930s (Kessener and Ribbius, 1935), but were generally forgotten until the energy crisis of the 1970s increased the awareness for energy-efficient technologies. Prior to the 1980s, many plants were designed with an α of 0.8, which was considered as a "universal" α for all types of aeration systems. It has been shown that different aeration methods have different α, and for fine-pore diffusers, the initial α decreases over time in operation due to fouling or scaling (Rosso and Stenstrom, 2006). Furthermore, for fine-bubble systems, α is a function of process conditions such as the mean cell retention time (MCRT) or the airflow rate (Rosso et al., 2005).

Mass transfer depression caused by contaminants has long been observed (Mancy and Okun, 1960). Eckenfelder and Barnhart (1961) reported the effects of organic substances on mass transfer, showing that contamination as low as 15 mg/l of sodium lauryl sulphate (SDS) can reduce mass transfer coefficients to 0.5 times the value in clean water. The effects of wastewater contamination on mass transfer can be related to the decrease in dynamic surface tension (McKeown and Okun, 1961; Masutani and Stenstrom, 1991). The interfacial accumulation of surfactants causes an increase in interfacial rigidity (hence in the drag coefficient), the reduction of internal gas circulation, and interfacial renewal rates. These gas–liquid interfacial phenomena have been recently discussed by the authors (Rosso, 2005).

The goal of this paper is to analyse contamination effects on gas–liquid interfaces due to surfactants, and compare them for the two cases of high and low interfacial velocities. In wastewater treatment, these regimes correspond, respectively, to coarse-bubble and surface aerators, and fine-pore diffusers. This paper summarizes previously observed phenomena, and explains the microscopic phenomena that cause different contamination effects at different flow regimes. The results of two laboratory studies using dynamic surface tension measurements and several other laboratory- and full-scale studies verify the conclusions. These results, along with our previously published work on the impact of MCRT and ageing or fouling on aeration efficiency, will be useful for aeration system design.

2. Materials and methods

Fig. 1 shows a generic drawing of the aeration apparatus used for the aeration studies, which was well-mixed and without dead zones. Aeration tests were performed according to the American Society of Civil Engineers (ASCE, 1984, 1991) standard. Dissolved oxygen (DO) was recorded over time in a solution where oxygen is first sequestered with sodium sulphite, using cobalt chloride as a catalyser. DO was measured with a YSI 58 DO meter (Yellow Springs Instruments, Yellow Springs, OH), and recorded via a NI DAQ-6015 (National Instruments, Austin, TX) acquisition board connected to a computer. For each measurement, airflow rate and dynamic wet pressure (i.e. the headloss across the aerator) were also collected. The experiments were performed with a single-bubble orifice and with a porous ceramic stone. The bubble size distribution was contained within a narrow range of diameters, and the arithmetic mean of sampled diameters was taken. Photographs of the process at high (1/500 s) and low (1/60, 1/125 s) shutter speed were taken, and used to observe and calculate bubble mean diameters and rise velocities.

The ASCE DO Parameter Estimation Program (DO_PAR 1.08, ASCE 1997; downloaded from: http://fields.seas.ucla.edu/research/dopar/) was utilized to calculate volumetric mass transfer coefficients (k_La, $time^{-1}$), oxygen transfer rates in standard conditions (SOTR, $mass_{O_2}/time$), oxygen transfer efficiency in standard conditions for clean water (SOTE, %), and oxygen transfer efficiency for surfactant solutions (αSOTE, %). The α-factor can be calculated as the ratio of process- to clean-water SOTE, i.e. αSOTE/SOTE. Previous investigations from our laboratory were also included (Masutani and Stenstrom, 1991; Huo, 1998).

A dimensional analysis was performed using the method by Zlokarnik (2002). The physical quantities included in the analysis are reported in Table 1. Due to low shear rate, in this process, the liquid viscosity has no influence. Highly viscous systems need a different dimensional analysis, because the transport phenomena occurring in these systems are due to different transport mechanisms. All other consideration on the statement of the problem are discussed in detail elsewhere (Rosso, 2005). The resulting seven dimensionless numbers and their physical significance are reported in Table 2. Π_1, $(\Pi_2)^{-1}$, and Π_7 can be recognized as the interfacial Sherwood (*Sh*), Bond (*Bd*), and Péclet (*Pe*) numbers, respectively. For clarity, Π_3, Π_5, and Π_6 are named the dimensionless characteristic length d^+, time t^+, and diffusivity D^+. Π_4 is named the gravitational contamination number (*Sm*). The problem is fully defined by the Π-set:

$$(Sh) = f\{(Pe), (Bd), (Sm),\ t^+,\ d^+,\ D^+\}. \quad (1)$$

The oxygen diffusivity at the surface is the sole time-dependent diffusivity used in this analysis. The surfactant bulk diffusivity is used in the analysis and the effects on the interface are reflected to the gas transfer by including the time-dependent dynamic surface tension. The use of a time-dependent surfactant diffusivity in the analysis will result in redundancy and in no improvement of statistical significance, as the time-dependent interfacial surfactant diffusivity is

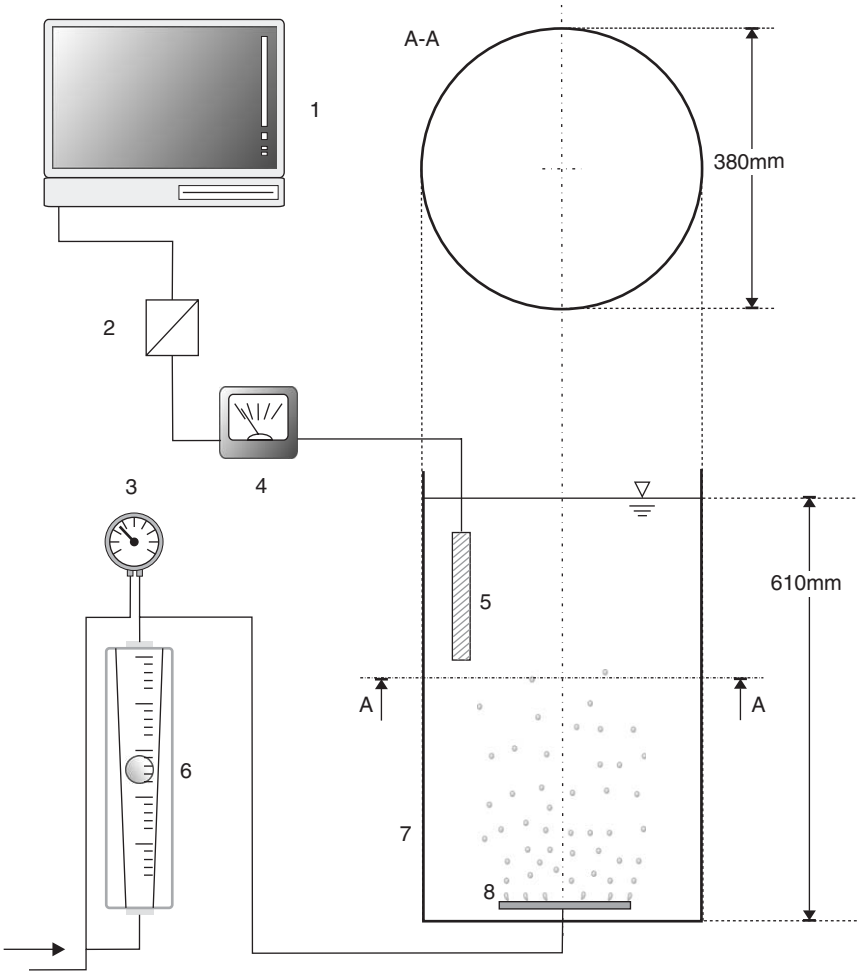

Fig. 1 – Aeration apparatus: (1) data logger, (2) D/A converter, (3) pressure gauge, (4) DO meter, (5) DO probe, (6) rotameter, (7) aeration tank, and (8) aerator.

Table 1 – Dimensionless analysis: physical quantities

$k_L a$ (t_B)	**Volumetric mass transfer coefficient**
d_B (t_B)	**Bubble diameter**
d_o	**Initial bubble (orifice) diameter**
$D_{s,O_2}(t_B)$	**Oxygen interfacial diffusivity**
$D_{B,SAA}$	Surfactant bulk diffusivity
$g\Delta\rho$	**Weight (i.e. buoyancy) of the bubble**
$\gamma(t_B)$	**Dynamic surface tension**
c_B	**Surfactant bulk concentration**
Q or u	Airflow rate or bubble velocity
t_B	Bubble age

calculated via a time-dependent model, function of the dynamic surface tension itself. The surfactant interfacial diffusivity was indeed calculated with the Ward–Tordai model (Ward and Tordai, 1946) to corroborate the results of the dimensional analysis, confirming the expectations that gas- and liquid-side diffusivities concurrently change with increasing time (Masutani and Stenstrom, 1991; Ferri and Stebe, 2000). The dimensionless length-scale d^+ was contained within a narrow range throughout our dataset, and showed no improvement of the regression analysis. Eq. (1) was reduced to

$$(Sh) = f\{(Pe), (Ro)\}, \tag{2}$$

where (Ro) is the surface contamination number, defined as

$$(Ro) = \frac{(Sm)}{(Bd)}(D^+)^2 t^+ = \frac{c_B t_B D_{B,SAA}^3}{\gamma d_B^3}. \tag{3}$$

The surface contamination number (Ro) represents the ratio of the surface contamination causes to the surface tension effects. Time-dependent contamination and surface tension are related differently for each contaminant. For example, two surfactants (one with high and one with low interfacial diffusivity) that depress surface tension to an equal equilibrium value have different (Ro) as they reach the equilibrium state in different time-scales. (Ro) differs from other dimensionless numbers that include surface tension, as it describes both the cause and the effect of the surface tension variations.

Table 2 – Dimensionless analysis: dimensionless numbers and their physical significance

Symbol	π-notation	Extended notation	Physical significance
(*Sh*)	Π_1	$\frac{k_L a d_B^2}{D_{s,O_2}}$	$\frac{\text{Mass diffusivity}}{\text{Molecular diffusivity}}$
(*Bd*)	$(\Pi_2)^{-1}$	$\frac{g\,\Delta\rho d_B^2}{\gamma}$	$\frac{\text{Gravity force}}{\text{Surface tension}}$
d^+	Π_3	$\frac{d_0}{d_B}$	Dimensionless length-scale
(*Sm*)	Π_4	$\frac{c_B D_{s,O_2}^2}{g\,\Delta\rho d_B^3}$	$\frac{\text{Surface contamination}}{\text{Gravity force}}$
t^+	Π_5	$\frac{t_B D_{s,O_2}}{d_B^2}$	$\frac{\text{Geometrical time scale}}{\text{Diffusional time scale}}$
D^+	Π_6	$\frac{D_{B,SAA}}{D_{s,O_2}}$	Dimensionless diffusivity
(*Pe*)	Π_7	$\frac{Q}{d_B D_{s,O_2}}, \frac{u d_B}{D_{s,O_2}}$	$\frac{\text{Advective forces}}{\text{Diffusive forces}}$
(*Ro*)	$\Pi_2\Pi_4\Pi_6^2\Pi_5$	$\frac{c_B t_B D_{B,SAA}^3}{\gamma d_B^3}$	$\frac{\text{Surface contamination (time)}}{\text{Surface tension (time)}}$

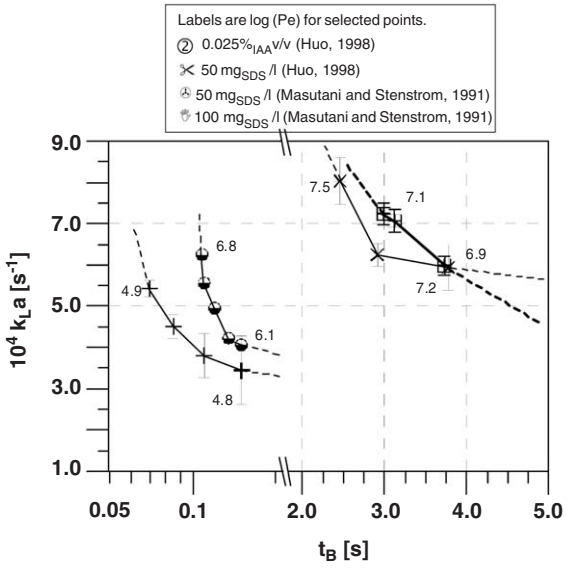

Fig. 2 – Evolution of mass transfer coefficients over increasing bubble surface age t_B. Labels are log(*Pe*) for selected points calculated at the interface, where liquid-side diffusivities are higher than bulk values.

Nonlinear regression analyses were performed using SYSTAT 10 (SPSS Corporation, Chicago, IL).

3. Results and discussion

Fig. 2 shows the evolution of mass transfer coefficients with increasing time. As time elapses, surfactant molecules migrate towards the surface, and hinder the interfacial renewal process, resulting in a rapid decrease in the volumetric mass transfer coefficient k_La, which is the product of liquid film coefficient, k_L, and interfacial area (a). Since bubbles are stable at smaller diameters in contaminated waters, the interfacial specific area is higher. Since k_La decreases, k_L must decrease more rapidly than the interfacial area (a) increases. Eckenfelder and Barnhart (1961) observed that k_L decreases with increasing surfactant concentrations, but k_La is minimum at low surfactant concentrations, and partially recovers at higher concentrations. This is the effect of a larger interfacial area (a), but reduced liquid film coefficient k_L.

In the case of moving interfaces, as for diffused and surface aerators, turbulence exists behind the interfacial laminar films. The Reynolds number is defined as

$$(Re) = \frac{du}{\upsilon}, \tag{4}$$

where d is the characteristic length, u the velocity, and υ the kinematic viscosity.

At a given interfacial flow regime, hence at a given interfacial (*Re*), the film renewal rate is decreased with increasing contamination, and lower internal gas circulation rates in bubbles (Garner and Hammerton, 1954). Roy and Duke (2004) photographed two-dimensional DO concentration gradients near surfaces contaminated with Triton X-100, showing reduced circulation outside contaminated bubbles, with lower interfacial O_2 concentration gradients for higher contaminations.

The intuitive concept of "molecular obstruction" is usually considered the cause of mass transfer depression. This phenomenon is dominant for stagnant gas–liquid interfaces, with zero interfacial fluid velocity, when molecular diffusion through the stagnant film is the only transport mechanism. For moving interfaces, turbulent transport towards the interface is the driving force for mass transfer, for two reasons: interfacial renewal rates and actual area covered by the surfactant molecules.

Higher contaminations with lower surface tensions cause higher boundary layer thickness, creating lower probability for turbulent eddies to reach the interface and carry "fresh" bulk fluid gas packets, causing lower renewal rates. Fig. 2 shows different mass transfer coefficients at same contaminations (50 mg_{SDS}/l). The higher mass transfer coefficients from higher interfacial velocities (characterized by higher interfacial Péclet numbers) are shown in Fig. 2. The same contaminations yield different mass transfer coefficients in different flow regimes; furthermore, higher interfacial velocity results in mass transfer coefficients in the same range,

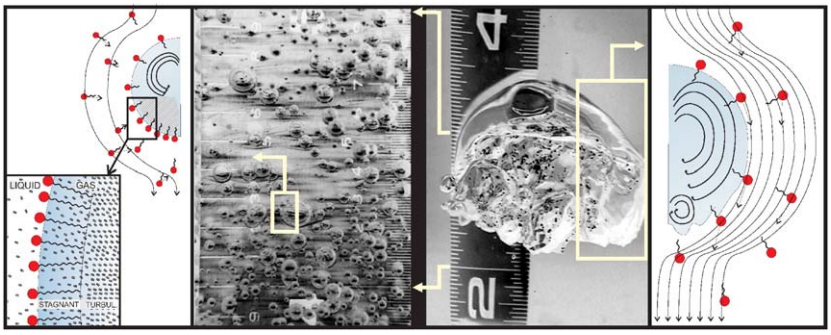

Fig. 3 – Comparison of fine (left photograph) and coarse (right photograph) bubbles generated by two different aerators operating at same airflow rate in the same surfactant solution (50 mg_{SDS}/l). The outer illustrations show the different mechanisms of interfacial accumulation in the two cases. The measuring scale is in inches (1 in = 25.4 mm), and each scale sub-division is 1/10 in (= 2.54 mm).

higher in average value than the range of mass transfer coefficients at low interfacial velocity. Therefore, the molecular obstruction phenomenon has a negligible effect on this mass transfer process.

Another consideration about the molecular obstruction theory is the effective diffusional area available for O_2 molecules to travel across the interface. Oxygen is present within the bubble at 20.95% mole fraction, while the surfactant accumulates on the bubble surface in much lower quantities. Furthermore, due to the nature of the surfactant, its polar head is anchored to the interface, and the hydrophobic tail is fluttering into the bubble volume. The molecular diameter for an oxygen molecule does not exceed 0.3 nm, while the diameter of the surfactant head is in the order of 10 nm or more. The frontal diameter to account for the surfactant is the diameter of the polar head, as the hydrophobic tails are inside the bubble, where gas molecules are free to move by virtue of molecular diffusion. If the molecular obstruction phenomena were dominant, reduced transfer should also occur for certain aliphatic alcohols, which show mass transfer enhancement ($\alpha > 1$), instead of depression (Zlokarnik, 1980). The interfacial accumulation of surfactant molecules is different at different angles from the front stagnation point (i.e. the highest point of the rising bubble), and the ratio between fore- and aft-accumulation varies between 10 and 100 times at $(Pe) = 10^5$ (Ramirez and Davis, 1999). The interfacial ratio of surfactant to oxygen molecules for our tests exceeded 1/100 on average around the bubble and 1/1000 on the upper cap. The ratio was calculated as the ratio of the average number of O_2 molecules versus surfactant molecules per unit of interfacial area. The number of O_2 molecules was calculated from gas kinetics, and the surfactant molecules from the surface accumulation Γ. If molecular obstruction is assumed dominant, it should be the same for both high and low interfacial velocities. Nevertheless, mass transfer depression has a higher magnitude at lower interfacial velocities, confirming that molecular obstruction is negligible for flowing systems.

Fig. 3 contains photographs at 1/500 in of coarse and fine bubbles in a 50 mg_{SDS}/l solution, and shows the inner fluid dynamic patterns with illustrations. The photographs show that the large majority of bubbles have diameters less than 1 mm. Clean water tests without surfactant in analogous conditions produced bubble mean diameters of about 4 mm, larger than any bubble in left-half of Fig. 3. In Fig. 3, one fine and one coarse bubble are highlighted and their interior circulation pattern is sketched to the side. The accumulation of surfactant at the fine-bubble interface occurs in larger extent than for coarse bubbles, as the hydraulic residence time is longer, and surfactant molecules have longer time available for surface migration. Also, smaller bubbles have much lower interfacial velocity, and once the surfactants have absorbed to the surface, their hydrophobic tails inside the bubble reduce the internal gas circulation, acting like a baffle in a stirred reactor (Garner and Hammerton, 1954). Surface active agents accumulate at the bottom of the bubble, creating a stagnation zone inside the bubble. Evidence supports the existence of fore-and-aft symmetry in the concentration distribution at the interface (Clift et al., 1978; Ramirez and Davis, 1999).

Additional photographs at low shutter speed were used to calculate the bubble mean rise velocity, which is approximately 0.2 and 1.5 m/s for fine and coarse bubbles respectively. With large interfacial area and large mass transfer time, fine bubbles should have a very high k_La. Yet, mass transfer coefficients in surfactant solutions are smaller than in clean water, even though bubble diameters are larger in clean water. Therefore, the time available for mass transfer in clean water is reduced due to greater rise velocity. For coarse–bubbles, the differences between clean and process water transfer rates are reduced, due to higher interfacial velocity and higher turbulence.

Fig. 4 shows the decline in α for selected measurements. The horizontal axis on this graph shows the mean bubble age (t_B), which is the average hydraulic retention time of bubbles in the vessel. The measurement of k_La is performed according to the ASCE method with a series of bubbles re-aerating over a time-scale of minutes. The rate of decline in α is greater for surfactants with greater molecular diffusivity. Conversely, higher molecular weight surfactants, which generally have lower diffusivity, require greater time to migrate towards the bubble interface, resulting in less depression of the α for the same bubble age. Also, higher interfacial flow velocities resist the decline in α caused by surfactant accumulation, due to the higher interfacial renewal rates.

Fig. 5 shows results for selected time-dependent interfacial accumulation tests in dimensionless form (Rosso et al., 2005). Data points in this plot are selected measurements, and trendlines are power best-fits to data with Eq. (5). The surfactant solution for this case was SDS in concentration of 50 mg/l, and the interfacial flow velocity was low ($u_B \sim 2 \times 10^{-2}$ m/s). The dimensionless time-scale t^+ represents early stages of interface life, which in dimensional terms ranges from 7×10^{-2} to 1.5×10^{-1} s. The evolution of mass transfer with increasing time is plotted as $(Sh) = f(t^+)$. After a rapid decrease, (Sh) tends to a minimum, which occurs at surface equilibrium. Concurrently, (Pe) decreases rapidly at first, reaching a plateau earlier than (Sh), because while (Pe) approaches a steady value ($t^+ > 2 \times 10^{-5}$), the contamination number (Ro) is still increasing. (Ro) represents surface contamination, which for this specific case is not completed at $t \sim 10^{-1}$ s. In dimensionless terms, (Ro) reaches a plateau for $t^+ > 5 \times 10^{-5}$ (for clarity, (Ro) is plotted in log-linear scale). In this time range, (Sh) also reaches a plateau.

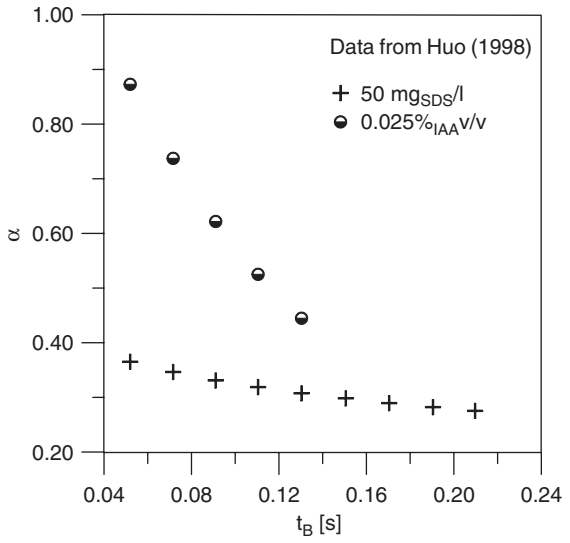

Fig. 4 – Evolution of α-factors over increasing bubble surface age t_B. The two datasets were measured with single-bubble testing apparatuses, utilizing solutions of sodium dodecyl sulphate (SDS) and iso-amyl alcohol (IAA).

The data was fit using the following equation:

$$(Sh) = \frac{0.382(Pe)^{1/3}}{1 + \log[1 + 10^{19}(Ro)]}. \quad (5)$$

Eq. (5) is statistically significant ($R^2 > 0.8$; $t > 10$; $P < 10^{-3}$; unbiased residuals). The numerator of Eq. (5) is a version of the well-known Frössling equation, which predicts mass transfer as a function of advection and diffusion in pure liquid systems (Frössling, 1938). Eq. (5) represents a modification of the Frössling equation for the case of contaminated solutions.

Fig. 6 shows the evolution of α with increasing (Re) and compares them to other types of aeration. For fine-pore diffusers, (Re) was calculated using the equivalent wet diameter of the bubble column over the diffusers d_{eq}, scaled for the volume fraction ϕ of liquid in the column. Coarse-bubble experiments were performed with a single nozzle, and (Re) was calculated for a single coarse bubble using the bubble diameter d_B as characteristic length. Data from Eckenfelder and Ford (1968) were included in Fig. 6 and show α for turbines

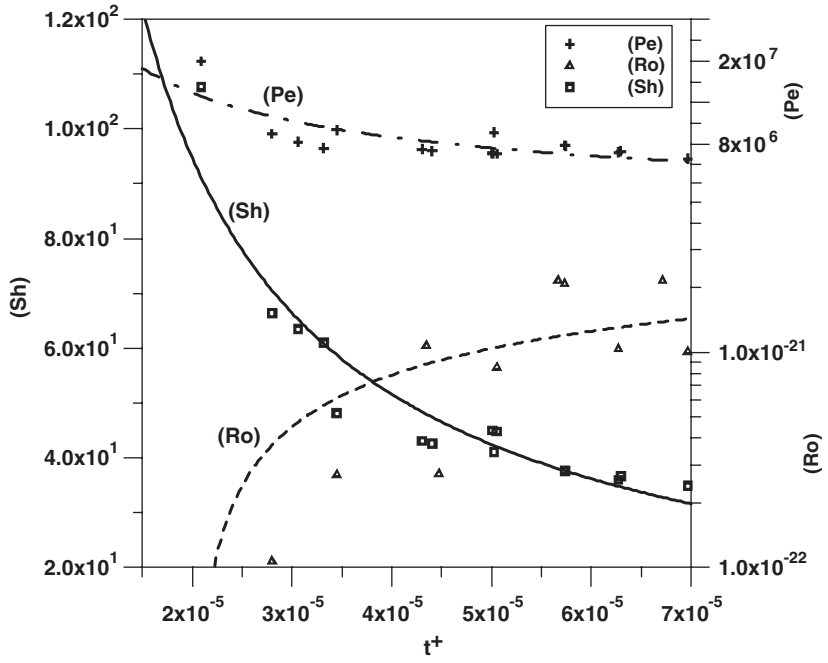

Fig. 5 – Dimensionless characterization of mass transfer phenomena at a fine-bubble interface at short-time limits. (*Sh*), (*Pe*), and (*Ro*) are the interfacial Sherwood, Péclet, and contamination numbers, respectively. Trendlines are power best-fits to data estimated with Eq. (5).

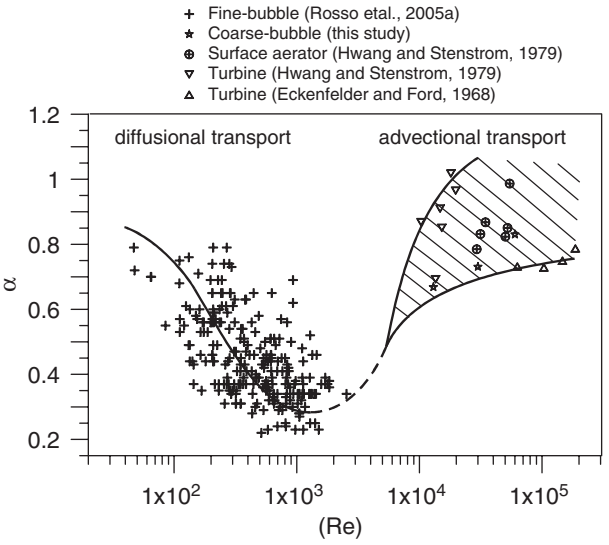

Fig. 6 – α-factors at different interfacial flow regimes. The shaded area represents a region of possible trendlines parametric in the energy density.

at different rotation regimes. For these data, (*Re*) was calculated for a droplet with diameter d_D of 5 mm travelling in the air at 5 m from the turbine shaft. Eq. (6) summarizes the definition of characteristic lengths for the three cases above:

$$d = \begin{cases} d_{column} = \frac{d_{eq}}{\phi} \rightarrow \text{for fine bubbles} \\ d_{bubble} \rightarrow \text{for coarse bubbles} \\ d_{droplet} \rightarrow \text{for surface aerators.} \end{cases} \quad (6)$$

The trendline in Fig. 6 confirms the behaviour of α versus turbulence predicted by Eckenfelder and Ford (1968). The dashed portion of the trendline shows an interfacial flow regime that is usually not encountered in aeration systems.

Viscous-flow domains [with $(Re)<10$] are usually not encountered in wastewater practice, with the possible exception of membrane bioreactors (Wagner et al., 2002). In this region, there is practically no effect of flow on α, as the gas transfer resistance is due primarily to the transport within the bulk liquid. In the transitional-flow domain, where fine-bubble aerators operate, an increase in (*Re*) results in a decline in α. Within this region [$50<(Re)<5000$], gas transfer is controlled by the surfactant interfacial migration, higher at higher (*Re*). In the laminar regime, i.e. the domain of fine-bubble diffusers, an increase of (*Re*) results in an increase of surfactant transport to the interface, hence a decrease in α. As (*Re*) increases into the turbulent regime, the surface renewal rate becomes high enough to shear surfactants off the surface, which increases the α-factor.

Coarse-bubble diffusers, jets, and surface aerators have a regime in the inertial-flow domain. For these gas–liquid interfaces, the higher range of (*Re*) results in higher interfacial renewal rates, and lower interfacial surfactant accumulation. The trendline shows that at very high (*Re*), α can be restored, and if the energy density is sufficient, values of α larger than 1.0 are possible (Zlokarnik, 1980). The reasons for the higher α include ionic interfacial effects due to the presence of inorganic salts, such as in seawater, or of some concentrated aliphatic alcohols (Zlokarnik, 1980). Another reason is the entrainment of foam created by surfactants. Such foams are either ephemeral or do not exist without surfactants. These foams can be stable and composed of fine-bubble aggregates with high interfacial areas. Operations at these conditions have low aeration efficiency, since values of α approaching or higher than 1.0 may be reached only at the expense of additional energy.

At extremely high energy densities, corresponding to $(Re)>10^5$, the higher interfacial shear rate reduces the thickness of the laminar film. At the upper limit, the interfacial resistant film will reduce its thickness to a few layers of water molecules, and the phenomenon of liquid vaporization will be dominant, as when turbines or pumps cavitate.

The cross-hatched area in Fig. 6 corresponds to a region where mass transfer is affected by local energy density. In this region, (*Re*) and the energy density may be independent and produce different mass transfer rates. For example, the results from Hwang and Stenstrom (1979) were collected in a small vessel with higher energy density while the results from Eckenfelder and Ford (1968) were collected in a large vessel. This phenomenon creates a range of α using experimental set-ups where (*Re*) and energy density are not controlled (Bass and Shell, 1977).

4. Conclusions

Turbulence controls gas transfer depression caused by surfactants, which is often quantified by α. Turbulence can be characterized by the interfacial Reynolds or Péclet numbers and the gas transfer by the interfacial Sherwood number. The Sherwood number can be correlated to the Péclet number to account for turbulence and to a dimensionless number, called the interfacial contamination number, to account for interfacial contaminant accumulation. The final correlation agrees with observed oxygen transfer rates.

Results explain why fine-bubble diffusers have greater mass transfer depression than coarse-bubble or surface aerators. The high turbulence associated with coarse-bubble aerators makes them behave more like surface aerators than fine-bubble aerators. High-turbulence aerators may achieve better transfer rates, but at the expense of greater energy density, and lower aeration efficiency (kg_{O_2}/kWh). Results also describe the variability of α measured at small scale, due to uncontrolled energy density.

REFERENCES

American Society of Civil Engineers—ASCE, 1984, 1991. Measurement of Oxygen Transfer in Clean Water. ASCE 2-91, American Society of Civil Engineers, New York.

Bass, S.J., Shell, G.L., 1977. Evaluation of oxygen transfer coefficients of complex wastewaters. In: Proceedings of the 32nd Industrial Waste Conference, Purdue University, Lafayette, IN.

Clift, R., Grace, J.R., Weber, M.E., 1978. Bubbles, Drops and Particles. Academic Press, New York.

Côté, P., Bersillon, J.-L., Huyard, A., 1989. Bubble-free aeration using membranes: mass transfer analysis. J. Membr. Sci. 47, 91–106.

Eckenfelder, W.W., Barnhart, E.L., 1961. The effect of organic substances on the transfer of oxygen from air bubbles in water. AIChE J. 7 (4), 631–634.

Eckenfelder, W.W., Ford, D.L., 1968. New concepts in oxygen transfer and aeration. In: Gloyna, E.F., Eckenfelder, Jr., W.W. (Eds.), Advances in Water Quality Improvement. University of Texas Press, Austin, TX, pp. 215–236.

Ferri, J.K., Stebe, K.J., 2000. Which surfactants reduce surface tension faster? A scaling argument for diffusion-controlled adsorption. Adv. Colloids Interface Sci. 85, 61–97.

Frössling, N., 1938. Über die Verdunstung fallender Tropfen. Gerlands Beitr. Geophys. 52, 170–215.

Garner, F.H., Hammerton, D., 1954. Circulation inside gas bubbles. Chem. Eng. Sci. 8 (1), 1–11.

Huo, D.L., 1998. The effect of dynamic surface tension on oxygen transfer coefficient in fine bubble aeration system. Ph.D. Thesis, University of California, Los Angeles.

Hwang, H.J., Stenstrom, M.K., 1979. The Effect of Surface Active Agents on Oxygen Transfer. UCLA-ENG-79-30, University of California, Los Angeles.

Kessener, H.J., Ribbius, F.J., 1935. Practical activated sludge research. J. Proc. Inst. Sew. Purification 6 (3), 50–56.

Mancy, K.H., Okun, D.A., 1960. Effects of surface active agents on bubble aeration. J. Water Pollut. Control Fed. 32 (4), 351–364.

Masutani, G., Stenstrom, M.K., 1991. Dynamic surface tension effects on oxygen transfer. J. Environ. Eng. 117 (1), 126–142.

McKeown, J.J., Okun, D.A., 1961. Effects of surface-active agents on oxygen bubble characteristics. Int. J. Air Water Pollut. 5 (2–4), 113–122.

Ramirez, J.A., Davis, R.H., 1999. Mass transfer to a surfactant-covered bubble or drop. AIChE J. 45 (6), 1355–1358.

Reardon, D.J., 1995. Turning down the power. Civ. Eng. 65 (8), 54–56.

Rosso, D., 2005. Mass transfer at contaminated bubble interfaces. Ph.D. Thesis, University of California, Los Angeles.

Rosso, D., Stenstrom, M.K., 2006. Economic implications of fine pore diffuser aging. Water Environ. Res. in press.

Rosso, D., Iranpour, R., Stenstrom, M.K., 2005. Fifteen years of off-gas transfer efficiency measurements on fine-pore aerators: key role of sludge age and normalized air flux. Water Environ. Res. 77 (3), 266–273.

Roy, S., Duke, S.R., 2004. Visualization of oxygen concentration fields and measurement of concentration gradients at bubble surfaces in surfactant-contaminated water. Exp. Fluids 36, 654–662.

Stenstrom, M.K., Gilbert, R.G., 1981. Effects of alpha, beta and theta factors in design, specification and operations of aeration systems. Water Res. 15, 643–654.

Wagner, M., Cornel, P., Krause, S., 2002. Efficiency of different aeration systems in full scale membrane bioreactors. In: Proceedings of 75th WEFTEC Conference, Chicago, IL.

Ward, A.F.H., Tordai, L., 1946. Time-dependence of boundary tensions of solutions I. The role of diffusion in time-effects. J. Chem. Phys. 14, 453–461.

Water Environment Federation—WEF, 1991. Design of Municipal Wastewater Treatment Plants—WEF Manual of Practice No. 8. WEF, Alexandria, VA.

Zlokarnik, M., 1980. Koaleszenzphänomene im System gasförmig/flüssig und deren Einfluß auf den O_2-Eintragbei der biologischen Abwasserreinigung. Korresp. Abw. 27 (11), 728–734.

Zlokarnik, M., 2002. Scale-Up in Chemical Engineering. Wiley-VCH, Weinheim.